

Simulation of non-Abelian Anyons using ribbon operators connected to a common base site

Xi-wang Luo, Yong-jian Han, Guang-can Guo, Xingxiang Zhou* and Zheng-wei Zhou†

A convenient and effective way in the quantum double model to study anyons in a topological space with a tensor product structure is to create and braid anyons using ribbon operators connected to a common base site [A. Kitaev *Ann. Phys. (N.Y.)* **303**, 2 (2003)]. We show how this scheme can be simulated in a physical system by constructing long ribbon operators connected to a base site that is placed faraway. We describe how to move and braid anyons using these ribbon operators, and how to perform measurement on them. We also give the smallest scale of a system that is sufficient for proof-of-principle demonstration of our scheme.

PACS numbers:

I. INTRODUCTION

Anyons are exotic quasi-particles in two dimensional systems that obey fractional statistics [1]. By the associative properties of their underlying algebra, they are divided into Abelian and non-Abelian anyons. Under particle exchange, the wavefunction of Abelian anyons acquires a phase that can be different than multiples of π . For non-Abelian anyons, the wavefunction is subject to a none diagonal unitary gate when two particles are exchanged [1, 2]. Anyons are important for understanding the physics of two-dimensional strongly correlated systems and they are speculated to exist in fractional quantum Hall fluids [3–5].

Aside from their fundamental implications in many-body physics, in recent years anyon systems have been suggested as a promising candidate for realizing intrinsically robust quantum computation because of their topological properties [6]. For instance, Kitaev proposed two exactly solvable spin lattice models with anyonic excitations, the quantum double model and the honeycomb model [6, 7]. These schemes are called topological quantum computation (TQC), and they take advantage of the topological invariance of anyon qubits to protect against local noise.

In spite of the conceptual significance of anyons and their appeal for quantum computation applications, it is very difficult to study anyons experimentally because the conditions for their existence and observation are extremely challenging to realize. To date, there has only been some experimental evidence in support of the existence of Abelian anyons in fractional quantum Hall fluids [3–5]. For the purpose of universal TQC, Abelian anyons are insufficient and non-Abelian anyons must be available. There have been several theoretical proposals for direct observation of non-Abelian anyons in quantum Hall systems [8, 9] and the honeycomb model [10–12]. Unfortunately, these proposals require very complex setup or very low temperatures that are beyond the reach of current experimental capabilities.

Considering the difficulty in realizing physical systems with genuine anyonic particles, quantum simulation of anyons is very valuable since it provides a viable alternative for studying the kinematics of topological states. In this practice, we will not try to construct the complex many-body Hamiltonian giving rise to genuine anyons which often involves interactions between more than two physical particles. Rather, the goal is to find practical methods to create topological states in a realizable system and study their properties. Though these states are not truly topologically protected, they can be created, manipulated and observed in a properly designed simulation system, and therefore are very valuable for the study of anyon physics and topological quantum computing.

Recognizing the importance of quantum simulation of anyon physics, in recent years researchers have proposed schemes for simulating both the Abelian [13, 14] and non-Abelian [15–17] quantum double model based on photonic and trapped atomic systems. Though these schemes are very valuable for the research of anyon physics, they also have serious limitations. In particular, the issue of using topologically protected manipulations only has not been sufficiently addressed. For instance, local fluxes and local charges are used in [16] to encode quantum information and these local degrees of freedom will be disturbed by local noise such as local gauge transformations. In [18], though information in the quantum memory is encoded with anyon states, the computing operations are non-topological. Therefore, it is necessary to study new schemes that can demonstrate genuine fractional statistics and simulate topologically protected quantum computing.

*Electronic address: xizhou@ustc.edu.cn

†Electronic address: zwzhou@ustc.edu.cn

In order to simulate anyon states that can truly demonstrate non-Abelian statistics and universal TQC, we must carefully examine the topologically protected space in the system which is the computational Hilbert space for TQC. In general, this topologically protected space does not have a tensor product structure and unitary transformations of states in it under braiding cannot be described clearly. Consequently, it is unclear how non-Abelian statistics is manifested in this space and how it can be used for computation [6]. To overcome this difficulty, Kitaev suggested that one can use an arbitrary but fixed *base site* as a reference [6] to create anyons. By constructing appropriate ribbon operators that share the chosen base site as one of their ends (see Fig. 2 (a)), one can create anyonic excitations on the other end of the ribbons. Since all these anyonic excitations have the same reference base site, an overall topologically protected space can be constructed as a tensor product of the topologically protected space associated with each ribbon operator [6]. The corresponding Hilbert space does have a tensor product structure and the transformations of anyon states in it under braiding and fusion can be easily derived. Kitaev's scheme offers a feasible and effective method for performing topologically protected quantum computation. Unfortunately, a scheme to directly simulate this important approach of Kitaev's has not been available, since it is nontrivial to construct appropriate ribbon operators required for its realization in a physical system.

In this work, we show how to dynamically simulate the S_3 non-Abelian quantum double model by proposing a scheme to realize ribbon operators connected to a common base site x_0 . We describe how to create anyonic excitations using these ribbon operators, and how to move the other end of the ribbon to achieve the braiding of anyonic excitations on it. We also demonstrate how to detect the braiding and fusion, and propose a method to realize anyonic interferometry using controlled ribbon operators to detect the topological states of the anyonic excitations. With these capabilities, we can then study the fractional statistics of non-Abelian anyons in the quantum double model, and also simulate universal TQC. Based on this, we investigate the minimum scale of a system that is required for proof-of-principle demonstration of our scheme, and propose an implementation using superconducting circuits.

II. THE QUANTUM DOUBLE MODEL

Kitaev's quantum double model is a spin Hamiltonian which is a sum of quasi-local operators in a two-dimensional lattice [6]. Its ground states are invariant under gauge transformations generated by some finite group. In this work, we consider the non-Abelian group $G = S_3$. For the convenience of discussion and without loss of generality, we focus on a square lattice as shown in Fig. 1. Particles live on the edges of the lattice, and their internal Hilbert space is described by the group G , $\mathcal{H} = \{|g\rangle : g \in G\}$. In Fig. 1, arrows are used to label the orientation of the edges in the lattice. Reversing the direction of a particular arrow is equivalent to making the basis change $|z\rangle \rightarrow |z^{-1}\rangle$ (where $|z\rangle \in \mathcal{H}, z \in G$) for the corresponding qudit. To describe the model, one need to define four types of linear operators acting on the Hilbert space \mathcal{H} : $L_{\pm}^g, g \in G$ and $T_{\pm}^h, h \in G$. Their effect on the basis state $|z\rangle$ is as follows:

$$L_+^g|z\rangle = |gz\rangle, L_-^g|z\rangle = |zg^{-1}\rangle, \quad (1)$$

$$T_+^h|z\rangle = \delta_{h,z}|z\rangle, T_-^h|z\rangle = \delta_{h^{-1},z}|z\rangle. \quad (2)$$

To study the effect of these operators on individual qudits, we use j and s to denote an edge of the lattice and one of its endpoints. Then one can define an operator $L_g(j, s)$ as follows: if s is the tail of the arrow on edge j then $L_g(j, s)$ is L_-^g acting on the j -th particle. If s is the head of the arrow on edge j , $L_g(j, s)$ is L_+^g acting on the same particle. Similarly, if p is the left (right) adjacent face of edge j then $T_h(j, p)$ is T_-^h (T_+^h) acting on the j -th particle. Local gauge transformations and magnetic charge operators for a vertex s and its adjacent face p are defined as

$$A_g(s, p) = A_g(s) = \prod_{j \in \text{star}(s)} L_g(j, s) \quad (3)$$

and

$$B_h(s, p) = \sum_{h_1 \cdots h_k = h} \prod_{m=1}^k T_{h_m}(j_m, p). \quad (4)$$

Here, $j_1 \cdots j_k$ are the boundary edges of face p , starting from and ending at vertex s and enumerated in the counter-clockwise direction. Notice that $B_h(s, p)$ is a projector into states with magnetic flux h on face p .

The quantum double model Hamiltonian defined by Kitaev is

$$H = \sum_s (1 - A(s)) + \sum_p (1 - B(p)), \quad (5)$$

where

$$A(s) = \frac{1}{|G|} \sum_g A_g(s), B(p) = B_e(s, p), \quad (6)$$

e is the identity element of the group. The ground states satisfy $A(s)|GS\rangle = |GS\rangle$, $B(p)|GS\rangle = |GS\rangle$ for all s and p , and excited states involve some violations of these conditions. Because the projection operators $A(s)$ and $B(p)$ are localized, excitations are particle-like living on vertices or faces, or both, where the ground state conditions are violated. A combination of a vertex and an adjacent face will be called a *site* (see Fig. 1).

A detailed examination of the excitation properties in the quantum double model is presented in [6]. Here, we just give a brief description sufficient for our purpose. The quantum double of group G , $D(G)$, is a quasi-triangular Hopf algebra that has a set of linear bases $D_{h,g}(x) = B_h(x)A_g(x)$ on site $x = (s, p)$. Though $D_{h,g}(x)$ is defined on each site, the structure of the quantum double does not depend on the *specific site*. Quasi-particle excitations in this system can be created by ribbon operators $F^{g,h}(r)$ introduced by Kitaev [6] which we will discuss in detail later. For a system with n quasi-particles, one can use $\mathcal{L}[n]$ to denote the quasi-particles' Hilbert space. By investigating how local operators $D_{h,g}(x) = B_h(x)A_g(x)$ act on this Hilbert space, one can define types and subtypes of these quasi-particles according to their internal states. It turns out that the types of the quasi-particles have a one-to-one correspondence with the irreducible representations of $D(G)$. These representations are labeled by $\Pi_{R(N_{[\mu]})}^{[\mu]}$, where $[\mu]$ denotes a conjugacy class of G which labels the magnetic charge. $R(N_{[\mu]})$ denotes a unitary irrep of the centralizer of an arbitrary element in the conjugacy $[\mu]$ and it labels the electric charge. The 8 irreps for $D(S_3)$ are listed in the Appendix.B. Once the types of the quasi-particles are determined they never change. Besides the type, every quasi-particle has a local degree of freedom, the subtype. The Hilbert space of n quasi-particles then splits according to $\mathcal{L}[n] = \bigoplus_{d_1 \dots d_n} \mathcal{K}_{d_1} \otimes \dots \otimes \mathcal{K}_{d_n} \otimes \mathcal{M}_{d_1 \dots d_n}$, where d_m is the type of the m th quasi-particle, and \mathcal{K}_{d_m} is the space of local degrees of freedom of the m -th quasi-particle. \mathcal{K}_{d_m} is just the representation spaces of $(\Pi_{R(N_{[\mu]})}^{[\mu]})_m$ and it is spanned by the basis $\{|\nu_{(L)}, \xi_{(L)}\rangle = |\nu_{(L)}\rangle \otimes |\xi_{(L)}\rangle\}$, where $\nu_{(L)} \in [\mu]_m$ and $|\xi_{(L)}\rangle$ is the basis of the representation space of $R(N_{[\mu]})_m$. $\mathcal{M}_{d_1 \dots d_n}$ is the topologically protected space. It is inaccessible by local measurements and insensitive to local perturbations. When we braid these quasi-particles, the protected space undergoes some unitary transformation, but the type and the subtype of the quasi-particles do not change under braiding.

Unfortunately, though $\mathcal{M}_{d_1 \dots d_n}$ is topologically protected, it does not have a tensor product structure. This makes it difficult to use it directly for quantum computation. However, if we choose a *base site* and connect it with other sites by non-intersecting ribbons (see Fig. 2 (a)), we can create quasi-particle excitations whose associated protected space can be described with a tensor product structure. Each quasi-particle excitation provides a protected subspace, and for a quasi-particle whose type is $\Pi_{R(N_{[\mu]})}^{[\mu]}$, the corresponding protected subspace is spanned by $\{|\nu, \xi\rangle = |\nu\rangle \otimes |\xi\rangle\}$, where $\nu \in [\mu]_m$ and $|\xi\rangle$ is the basis of the representation space of $R(N_{[\mu]})_m$. The overall topologically protected space is the tensor product of these protected subspaces. These quasi-particle excitations are non-Abelian anyons. Their braiding and fusion rules are given in [6, 19], and a brief summary of S_3 group and $D(S_3)$ anyons is given in the Appendix. If the conjugacy class $[\mu] = [e]$, where e is the identity group element, the quasi-particle is a pure electric excitation, we can simply use $|\xi\rangle = |(\nu, \xi)\rangle$ to denote its topological state. If the unitary irrep R is the identity representation, the quasi-particle is a pure magnetic charge excitation, and we use $|\nu\rangle = |(\nu, \xi)\rangle$ to denote its topological state. For these pure charge excitations, their local degrees of freedom can also be simplified in the same way. These pure charge excitations based on $D(S_3)$ are sufficient for universal TQC [20]. The braiding rules for pure charge excitations are

$$\mathcal{R}|\nu_1\rangle|\nu_2\rangle = |\nu_1\nu_2\nu_1^{-1}\rangle|\nu_1\rangle, \quad (7)$$

and

$$\mathcal{R}^2|\nu\rangle|\xi_n^R\rangle = |\nu\rangle|R(\nu)_{mn}\xi_m^R\rangle. \quad (8)$$

In the above equations, we have neglected the local degree of freedom. R is the unitary irrep of S_3 corresponding to pure electric charge excitation. ν corresponds to pure magnetic charge, and \mathcal{R} denotes the counterclockwise exchange of the two anyonic excitations. The exchange between pure electric charges is trivial.

III. SIMULATION OF THE QUANTUM DOUBLE MODEL

The quantum double Hamiltonian in Eq. (5) is very difficult to realize because it requires interactions between more than two particles. Instead of engineering a Hamiltonian with genuine multiparticle interactions, we take a dynamic

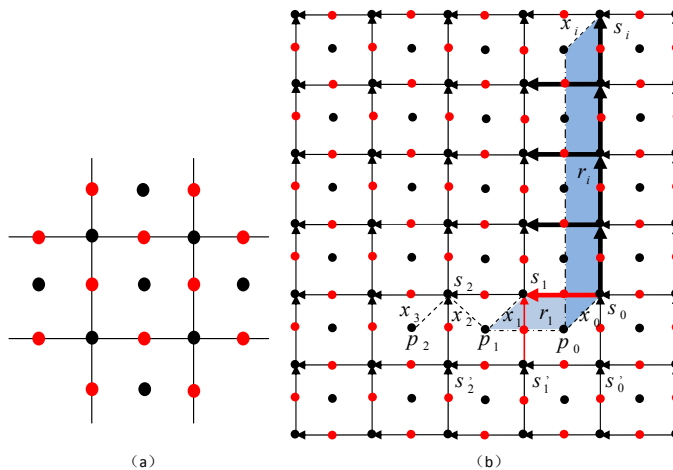


FIG. 1: (Color online)(a) A spin lattice for the quantum double model. The system particles (red) reside on the edges of the lattice. All particles on edges that meet at a vertex interact. Ancillary particles (black) reside on the vertices and center of the faces. They can interact with their nearest system particles. (b) Short and long ribbons on the lattice indicated by the blue areas. Arrows label the orientation of the edges. The short ribbon operator for ribbon r_1 connects adjacent sites x_1 and x_0 and acts on the two red edges. The long ribbon r_i connects faraway sites x_i (dashed) and the base site x_0 . The corresponding ribbon operator acts on the edges in thick lines.

approach to construct appropriate ribbon operators using local operations involving no more than two qudits at a time.

We focus on the square lattice model shown in Fig. 1. System qudits live on the edges. In previous schemes [15, 16] based on trapped atoms in 2d optical lattices, ancillary qudits are also used. They are not needed if the system qudits are addressable, as is the case in a solid-state system. Nevertheless, in order to demonstrate the wide applicability of our scheme, we will present it in a system with ancillary qudits that reside on the vertices and center of faces too (see Fig. 1 (a)). The ancillary qudits are assumed to be addressable.

To simulate the quantum double model, we apply single-qudit gates on individual ancillary qudits, as well as single-qudit gates on all system qudits simultaneously (since they are not addressable). In addition, we need the two-qudit diagonal phase gate $U = \exp(i\phi|g_i\rangle_A \langle g_i| \otimes |g_i\rangle_B \langle g_i|)$ between an ancillary qudit and its adjacent system qudits. With these operations, all two-qudit controlled rotations between the ancilla and system qudits can be constructed efficiently [16, 21].

A. Ground state preparation

We first need to prepare the system in the ground state, and this can be achieved using a similar method as in [15, 16]. Initially, all system qudits and face ancillary qudits are in state $|e\rangle$ and vertex ancillary qudits are in state $\frac{1}{\sqrt{|G|}} \sum_g |g\rangle$. Note that in this initial state, $B(p) = 1$ for all p . To create the ground state, we only need to make the symmetrized gauge transformation projection $A(s)$ Eq. (6) on every vertex. This symmetrized gauge transformation is carried out from left to right and top to bottom on all vertices in the lattice. The ground state is created as a result. Now we take s_0 in Fig. 1 (b) as an example and show how to make the projection $A(s_0)$. Projections $A(s)$ on other vertices are similar. Using the vertex ancillary qudit s_0 as the controlled qudit, we apply on system qudits the controlled gauge transformation $\sum_g |g\rangle_{s_0} \langle g| \otimes A_g(s_0)$. After this operation, the state of system qudit on edge $[s_0, s'_0]$ (i.e. the bottom edge of s_0 in Fig. 1 (b)) is the same as state of ancilla s_0 . Then, disentangle the ancillary qudits from the system by controlled two-qudit gate $\sum_g |g\rangle_{[s_0, s'_0]} \langle g| \otimes L_+^{g^{-1}}(s_0)$ between the system qudit on edge $[s_0, s'_0]$ and ancilla s_0 . Now the ancilla s_0 is in state $|e\rangle$, and we make the operation $A(s_0) = \frac{1}{\sqrt{|G|}} \sum_g A_g(s_0)$.

Alternatively, one can realize the above disentanglement step by first making proper measurements on the vertex ancilla, and then performing appropriate corrections on the system qudits according to the measurement outcome [16]. For the correction, one needs single qudit unitary operations on system qudits. Assuming one of the operations on single system qudit is U , without addressability of system qudits, we can still realize U by preparing an adjacent (and addressable) ancillary qudit a in the state $|h\rangle$ and performing the controlled unitary operation $|h\rangle_a \langle h| \otimes U + 1_{|G|-1} \otimes 1_{|G|}$. Similarly, all single-qudit operations on system qudits in our following schemes can be implemented by this technique.

B. Anyon creation and braiding

The central issue in our simulation is anyon creation from ground state. In order to create a topologically protected space with a tensor structure that can be used for TQC, we choose an arbitrary site x_0 as our base site as shown in Fig. 1 (b). The key then is to find ways to create anyons by dynamically performing the ribbon operators $F^{g,h}(r)$ connected to x_0 on the ground state (see Fig. 1 (b)). This will allow us to create arbitrary topological states of a given type by applying the superposition ribbon operator $\sum_{z \in S_3} \alpha_z F^{\mu,z}(r)$, where μ corresponds to the anyon type and α_z are the coefficients.

These ribbon operators $F^{g,h}(r)$ act as follows [6]

$$\begin{aligned}
 & \begin{array}{c} \xleftarrow{y_1} \xleftarrow{y_2} \xleftarrow{y_3} \\ \uparrow y'_1 \quad \uparrow y'_2 \quad \uparrow y'_3 \\ F^{(h,g)}(r) \end{array} \\
 = & \delta_{g, y_1 y_2 y_3} \begin{array}{c} \xleftarrow{y_1} \xleftarrow{y_2} \xleftarrow{y_3} \\ \uparrow h y'_1 \quad \uparrow y_1^{-1} h y_1 y'_2 \quad \uparrow (y_1 y_2)^{-1} h (y_1 y_2) y'_3 \end{array}
 \end{aligned} \tag{9}$$

The ribbon operators $F^{(h,g)}(r)$ commute with every projector $A(s)$ and $B(p)$, except when (s, p) is on either end of the ribbon. Therefore, the ribbon operator creates excitations on both ends of the ribbon. To simplify our discussion, we will use long ribbon operators to create excitations at sites (infinitely) far away from the base site x_0 . When one examines the excitations on these sites, the base site x_0 is at an (infinitely) faraway location, and one can ignore the effect of the excitations on the base site x_0 [6]. By doing so, when we apply a long ribbon operator connected to x_0 we can solely focus on the quasi-particle excitation on the other end of the ribbon [6].

In the spirit of this consideration, we will first propose a method to realize short ribbon operators to create anyons near the base site x_0 , and then show how to move them faraway from x_0 to implement a long ribbon operator. This protocol to move anyons around is needed for anyon braiding and measurement too, and thus is critical ingredient in our scheme.

Now let us study how to perform a short ribbon operator in the general superposition form

$$\sum_{z \in S_3} \alpha_z F^{\mu,z}(r_1),$$

where r_1 is a ribbon connecting the base site x_0 and a nearby site x_1 in Fig. 1 (b). This allows us to create an anyon at x_1 in an arbitrary topological state with a certain type determined by μ .

In order to perform the ribbon operator $\sum_{z \in S_3} \alpha_z F^{\mu,z}(r_1)$, we need the projection operation $\sum_i \alpha_{z_i} |z_i\rangle\langle z_i|$ ($z_i \in \{z \in G | \alpha_z \neq 0\}, i = 1, 2, \dots, m$) on system qudit $[s_0, s_1]$ and single qudit gate L_+^μ on system qudit $[s_1, s'_1]$. Using a single projection measurement that corresponds to operation $|g\rangle\langle g|$, together with appropriate gauge transformations, we can realize the projection $\sum_i \alpha_{z_i} |z_i\rangle\langle z_i|$:

$$\begin{aligned}
 & \sum_i \alpha_{z_i} A_{z_i}(s_1) A_{g_1^{-1}}(s_1) |g_1\rangle_{[s_0, s_1]} \langle g_1 | |GS\rangle \\
 = & \sum_i \alpha_{z_i} A_{z_i}(s_1) A_{g_1^{-1}}(s_1) |g_1\rangle_{[s_0, s_1]} \langle g_1 | A_{g_1} |GS\rangle \\
 = & \sum_i \alpha_{z_i} A_{z_i}(s_1) |e\rangle_{[s_0, s_1]} \langle e | A_{z_i^{-1}}(s_1) |GS\rangle \\
 = & \sum_i \alpha_{z_i} |z_i\rangle_{[s_0, s_1]} \langle z_i | |GS\rangle.
 \end{aligned}$$

We have used $A_g(s_1) \equiv 1$ as there is no excitation at vertex s_1 (i.e. $A(s_1) = 1$). Following this idea, we can design the following protocol to perform the ribbon operator $\sum_{z \in S_3} \alpha_z F^{\mu,z}(r_1)$.

1. Measure system qudit on edge $[s_0, s_1]$ in the basis $\{|g\rangle\}$. This is done by applying the two qudit unitary between system qudit on edge $[s_0, s_1]$ and ancillary qudit p_0 , $\sum_g |g\rangle_{[s_0, s_1]} \langle g| \otimes L_+^g(p_0)$, and then measuring ancilla p_0

in the basis $\{|g\rangle\}$. If the outcome is $|g_1\rangle$, perform gauge transformation $A_{g_1}^{-1}(s_1)$ (This step is equivalent to a projection $|e\rangle\langle e|$ on edge $[s_0, s_1]$).

2. Prepare the ancillary qudit s_1 in the state $|0_{[\alpha_z]}\rangle_{s_1} \propto \sum_i \alpha_{z_i} |z_i\rangle$ and apply the controlled gauge transformation $\sum_g |g\rangle_{s_1} \langle g| \otimes A_g(s_1)$.
3. Measure the ancillary qudit s_1 in the basis $\{|k_{[z]}\rangle = Z_{[z]}^k |0_{[z]}\rangle\}$, where $Z_{[z]}^k = \sum_{z_j} \exp(i2\pi k j/m) |z_j\rangle\langle z_j|$ and $|0_{[z]}\rangle = \frac{1}{\sqrt{m}} \sum_i |z_i\rangle$. For outcome $k_{[z]}$, apply the single qudit operation $Z_{[z]}^{k_{[z]}}$ on the system qudit on edge $[s_0, s_1]$ as a correction. Alternatively, this disentanglement step can be done by applying two-qudit gate $\sum_g |g\rangle_{[s_0, s_1]} \langle g| \otimes L_+^{g^{-1}}(s_1)$ between system qudit on edge $[s_0, s_1]$ and ancilla s_1 .
4. Apply operation $L_\mu(j, s_1)$, where j is the edge $[s_1, s'_1]$.

By these steps, we can create an anyon at x_1 with arbitrary type and topological state. We first take the pure magnetic charge excitation

$$|\mu_{(L)}; \nu\rangle = |C|^{\frac{1}{2}} \sum_{z \in G: z^{-1}\mu z = \nu} F^{\mu_{(L)}, z}(r_1) |GS\rangle$$

as an example. Here, $\mu_{(L)}$ is an element of the conjugacy class C . It corresponds to the magnetic flux at site x_1 and characterizes the local degree of freedom. ν , on the other hand, corresponds to the magnetic flux across a counterclockwise circle, starting and ending at the base site x_0 and surrounding only the quasi-particle at x_1 . It is the topological state that we are interested in. Notice that, for this pure magnetic charge anyon $|\mu_{(L)}; \nu\rangle$, the corresponding coefficients $\alpha_{z_i} \neq 0$ only when $z_i \in \{z \in G | z^{-1}\mu z = \nu\}$, and $\alpha_{z_i} = |C|^{\frac{1}{2}}$ for all $z_i \in \{z \in G | z^{-1}\mu z = \nu\}$. So, in step 2 given above, we prepare the ancillary qudit at s_1 in the state $|0_{[z]}\rangle_{s_1} \propto \sum_i |z_i\rangle$, with $z_i \in \{z \in G | z^{-1}\mu z = \nu\}$. As another example, we look at the pure electric charge excitation $|\xi_{(L)}; \eta\rangle = |R|^{\frac{1}{2}} \sum_{g_i} R_{\xi_{(L)}, \eta}(g_i) F^{e, g_i}(r_1) |GS\rangle$, where R is a irreducible representation of the group G (see the appendix), $\xi_{(L)}$ is the local degree of freedom, and η characterizes the topological state. To create this state, we need to prepare the ancillary qudit at s_1 in the state $|0_{[R_{\xi_{(L)}, \eta}]\rangle_{s_1} \propto \sum_{g_i} R_{\xi_{(L)}, \eta}(g_i) |g_i\rangle$ in step 2. As a more generic example, we look at the dyonic combination excitation $|\nu, \xi\rangle$ where ν and ξ are both topological degrees of freedom (local degrees of freedom ignored). To create this state, we perform corresponding superpositions of ribbon operators $\sum_{h \in S_3} \alpha_h F^{g, h}(r)$ with a fixed $g \in [\nu]$, and appropriate coefficients α_h determined by the topological state.

Once we created anyonic excitations on sites close to the base site x_0 , we need to move them far away from x_0 and also braid them. For these purposes, we need two basic movements. We need to move the excitation from the original site to an adjacent site sharing a common face, and from the original site to an adjacent site sharing a common vertex. In Fig. 1 (b), these correspond to moving the excitation from site x_1 to x_2 , and from x_2 to x_3 .

For the first quasi-particle movement from site x_1 to site x_2 , mathematically, this means mapping the group element corresponding to state for qudit $[s_0, s_1]$ to a product of group elements corresponding to states for qudits $[s_1, s_2]$ and $[s_0, s_1]$ (i.e. coherently mapping from $|g_1\rangle_{[s_0, s_1]} |g_2\rangle_{[s_1, s_2]} |\psi\rangle_{rest}$ to $|g'_1\rangle_{[s_0, s_1]} |g'_2\rangle_{[s_1, s_2]} |\psi'\rangle_{rest}$ with $g'_2 g'_1 = g_1$ and $|\psi\rangle_{rest}$ referring to the state of the qudits in the rest of the system) and moving the flux at x_1 to x_2 . To do this, we first perform the projection operation $|e\rangle\langle e|$ on the qudit on edge $[s_1, s_2]$ (see the first step of anyon creation). Now qudits $[s_1, s_2]$ and $[s_0, s_1]$ are in state $|g'_2\rangle_{[s_1, s_2]} |g'_1\rangle_{[s_0, s_1]}$ with $g'_2 = e$ and $g'_1 = g_1$, and we have $g'_2 g'_1 = g_1$. The flux at site x_1 doesn't change and now the flux at site x_2 is the same as site x_1 . Then, recall the action of the ribbon operator, we need to erase redundant excitation at site x_1 to finish this movement. This can be done by applying the symmetrized gauge transformation $A(s_1)$ in Eq. (6) at vertex s_1 (for operation $A(s_1)$, see the ground state preparation).

The second basic movement from site x_2 to x_3 has been studied in [16]. Here we give a similar scheme with a simpler disentanglement step. We first coherently map the flux at site x_2 to the ancillary qudit at p_1 by the controlled operation

$$\Lambda(x_2, p_1) = \sum_{g \in S_3} B_g(x_2) \otimes L_+^g(p_1).$$

Then we apply the controlled unitary $\sum_{h \in S_3} |h\rangle_{p_1} \langle h| \otimes L_+^{h^{-1}}([s_2, s'_2])$ to move the flux from site x_2 to site x_3 , just as in [16]. Finally we disentangle the ancillary qudit p_1 from the system by first swapping ancilla p_1 and p_2 and then applying $\Lambda(x_3, p_2)^{-1}$. The controlled operation $\Lambda(x, p)$ can be decomposed into elementary two-qudit controlled rotation operators with each edge surrounding p as a control and the ancilla as the target [16].

The combination of these two basic movements allows us to move any anyonic excitations around. By applying them repeatedly, we can realize a long ribbon and move the quasi-particle to an arbitrary site faraway from the base

site x_0 and also braid the anyons. Notice that, after we create an anyonic excitation at a location faraway from the base site x_0 , we can use the same procedure to create more anyonic excitations by first applying a short ribbon operator and then moving the excitation away. In this process, since the excitations created earlier have been moved away from around the base site, they will not affect the short ribbon operations later.

For TQC based on this quantum double model $D(S_3)$, two kinds of ancillary vacuum states are needed, the chargeless pair state of pure electric charges $|I_{|R|}\rangle = \frac{1}{\sqrt{|R|}} \sum_{\eta} |\eta\rangle_R \otimes |\eta\rangle_{R^*}$ and the chargeless pair state of pure magnetic charges $|I_{|\mu|}\rangle = \frac{1}{\sqrt{|\mu|}} \sum_{\nu \in |\mu|} |\nu\rangle \otimes |\nu^{-1}\rangle$ [20]. Here, η and ν are topological states and we omit the local degrees of freedom, and R is an irreducible representation of the group S_3 (see the appendix). The pair excitations localized at sites x_i and x_j (Fig. 2 (a)) can be created by a ribbon operator connecting x_i and x_j . If a pair of anyons is created from vacuum, the total topological charge of them is zero automatically. So we have $|I_{|R|}\rangle = |R|^{\frac{1}{2}} \sum_z R_{\xi_1(L)\xi_2(L)}(z) F^{e,z}(r_{i,j}) |GS\rangle$, and $|I_{|\mu|}\rangle = |C|^{\frac{1}{2}} \sum_{z:z^{-1}\mu_1(L)z=\mu_2(L)} F^{\mu_1(L),z}(r_{i,j}) |GS\rangle$, where $r_{i,j}$ is a ribbon that connects x_i and x_j , and $\xi_1(L)$, $\xi_2(L)$, $\mu_1(L)$ and $\mu_2(L)$ are all local degrees of freedom. Obviously, we can dynamically create this excitation pair by performing the corresponding ribbon operators using the method discussed earlier. Therefore, we can simulate universal TQC in principle.

C. Fusion and Topological state Measurements

We must be able to measure the anyon states in order to simulate the quantum double model. Measurement is also needed for TQC. An indirect but technically less challenging method is to perform a fusion measurement. It probes the fusion rules of the anyons by which we can confirm the topological nature of the system. If we want to study the braiding rules, then a direct measurement of anyons' topological states is necessary. These measurements can be accomplished by closed ribbon operator projection and interference.

There are a few ways to do a fusion measurement. One can first fuse two anyons to one and then measure the type of the new anyon. Alternatively, one can move two anyons close and perform appropriate closed ribbon operators that encircle them, which does not destroy the two anyons since they are not really fused. In our dynamical simulation, this is the realistic approach since we can only move two anyons close rather than fuse them.

For TQC, the only measurement we need is to detect whether there is a quasi-particle left or whether two anyons have vacuum quantum numbers when they fuse [20]. Assuming the closed ribbon c in Fig. 2 (b) encircles only the two anyons to be fused, this measurement corresponds to the projection ribbon operator [22]

$$\frac{1}{|G|} \sum_{g \in G} F^{g,e}(c) \quad (10)$$

which casts the two anyons into the vacuum quantum number state when they fuse. We then focus on this projection ribbon operator and show how to realize it. In principle, projection operators corresponding to other fusion channels can be realized in a similar way.

As shown in Fig. 2 (b), to make the projection in Eq.(10), all ancillary qudits are initially prepared in state $|e\rangle$. We first prepare ancillary qudit p_0 in state $|0_{[G]}\rangle = \frac{1}{\sqrt{|G|}} \sum_g |g\rangle$. And if we apply the controlled ribbon operator $\sum_{g \in G} |g\rangle_{p_0} \langle g| \otimes F^{g,e}(c)$, we get the final state of the system and ancilla p_0 : $|\psi_f\rangle \propto \sum_{g \in G} |g\rangle_{p_0} F^{g,e}(c) |\psi_i\rangle$. We can then measure p_0 in basis $\{|k_{[G]}\rangle = Z_{[G]}^k |0_{[G]}\rangle\}$, where $Z_{[G]}^k = \sum_{g_j} \exp(i2\pi k j / |G|) |g_j\rangle \langle g_j|$. If the outcome is $|0_{[G]}\rangle$, the projection in Eq. (10) succeeds, and the two anyons in ribbon c have vacuum quantum number when they fuse. If the outcome is not $|0_{[G]}\rangle$, the projection fails, and there is a quasi-particle left. The controlled closed ribbon operator can be realized by first performing a short controlled ribbon operator and then coherently moving one end of the ribbon along c until the ribbon is closed. Notice that $F^{g,e}(c)$ contains projections. And for the last two step movements that close the ribbon, there may be excitations at the target site of the movements, but our movement scheme above only works when there are no excitations at the target sites. So we must carefully close the ribbon. The following steps should be followed.

1. Prepare ancillary qudit p_0 in state $|0_{[G]}\rangle = \frac{1}{\sqrt{|G|}} \sum_g |g\rangle$. Perform the projection operation $|e\rangle \langle e|$ on the qudit on edge $[s_0, s_1]$ (see the first step of anyon creation).
2. Apply the controlled two-qudit gate $\sum_{g \in G} |g\rangle_{p_0} \langle g| \otimes L_g(s_1, [s_1, s'_1])$ between the ancillary qudit p_0 and system qudit $[s_1, s'_1]$.
3. Move the excitation at (s_1, p_1) along the ribbon c in the clockwise direction to site (s_n, p_n) in Fig. 2 (b).

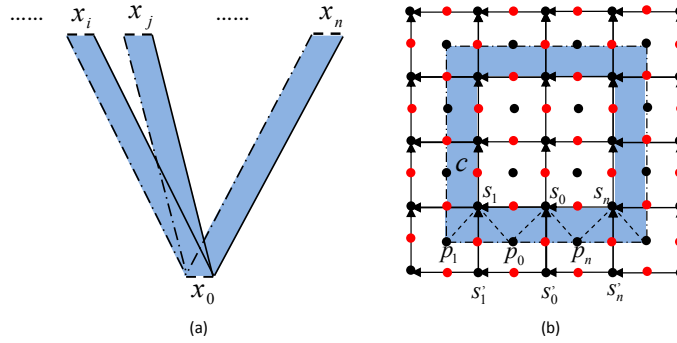


FIG. 2: (a) Non-intersecting ribbons with one common end x_0 (the base site). (b) A closed ribbon for fusion measurement.

4. Measure qudit $[s_n, s_0]$ in basis $\{|g\rangle : g \in G\}$. If the outcome is not $|e\rangle$, projection Eq.(10) fails and there is a quasi-particle left when the two anyons fuse. If the outcome is $|e\rangle$, perform $A(s_n)$ in Eq. (6).
5. Apply the controlled two-qudit gate $\sum_{g \in G} |g\rangle_{p_0} \langle g| \otimes L_g(s_0, [s_0, s'_0])$ between the ancillary qudit p_0 and system qudit $[s_0, s'_0]$. Measure ancillary qudit p_0 in basis $|k_{[G]}\rangle = Z_{[G]}^k |0_{[G]}\rangle$, where $Z_{[G]}^k = \sum_{g_j} \exp(i2\pi k j / |G|) |g_j\rangle \langle g_j|$. If the outcome is $|0_{[G]}\rangle$, the projection is done and the two anyons in ribbon c have vacuum quantum number when they fuse. Otherwise, there is a quasi-particle left behind.

Aside from fusion measurements, we can also measure the topological states of the anyons directly in an interference experiment. This can be accomplished by using controlled braiding. In Fig. 1 (b), assume we want to measure the anyon at site x_i which is in some unknown topological state $|x\rangle$. We make use of the ancillary anyon at site x_1 Fig. 1 (b) (assuming x_1 is faraway from the base site x_0) which is prepared in the topological state $|a\rangle$. To perform the interference measurements, initially, we prepare all ancillary qudits in state $|e\rangle$. Then

1. prepare the ancillary qudit p_1 in state $\frac{1}{\sqrt{2}}(|e\rangle + |h\rangle)$;
2. coherently braid the anyon at x_1 around x_i counterclockwise only when the ancillary particle p_1 is in state $|h\rangle$;
3. measure the ancilla p_1 in basis $\{\frac{1}{\sqrt{2}}(|e\rangle \pm |h\rangle)\}$.

The outcome of the measurement on the ancilla p_1 is $m = \pm 1$. The probability distribution for either result is

$$P(m = 1) - P(m = -1) = \text{Re}[\langle a | \langle x | \mathcal{R}^2 | x \rangle | a \rangle] \quad (11)$$

Therefore, changing the state $|a\rangle$ and measuring the probability distributions allows us to obtain the real part of the interference amplitudes. Similarly, measuring the ancilla p_1 in the basis $\{\frac{1}{\sqrt{2}}(|e\rangle \pm i|h\rangle)\}$ yields the imaginary part of the interference amplitudes. With these interference amplitudes, one can determine the topological state $|x\rangle$ [19].

The most critical step for the interference measurement is the controlled braiding. It can be realized by controlled movements of anyons and braiding operations. First, we coherently move the anyon at x_1 to x_3 if and only if the ancilla p_1 is in state $|h\rangle$. Then we braid anyon at x_3 around x_i . Finally, we perform a controlled movement of the anyon from x_3 back to x_1 .

For the controlled movement from x_1 to x_3 and back, we first perform the projection operation $|e\rangle \langle e|$ on the system qudit $[s_1, s_2]$. Now the product of group elements corresponding to states of qudits $[s_0, s_1]$ and $[s_1, s_2]$ is the same as group element corresponding to state of qudit $[s_0, s_1]$, and the flux at site x_2 is the same as site x_1 . Recall the action of ribbon operators, we can make a controlled erase of the quasi-excitations at x_2 and x_1 to finish this controlled movement. If the ancilla p_1 is in state $|e\rangle$, we erase the excitation at site x_2 by the symmetrized gauge transformation $A(s_2)$ Eq. (6) to cancel the movement. If the ancilla p_1 is in state $|h\rangle$, we erase the excitation at site x_1 by the symmetrized gauge transformation $A(s_1)$ in Eq. (6) to finish the movement. Assume the magnetic flux at site x_1 is μ_1^{-1} which is the local degree of freedom of the ancillary anyon, the controlled movement from site x_2 to x_3 is done by applying the operation $|e\rangle_{p_1} \langle e| \otimes I([s_2, s'_2]) + |h\rangle_{p_1} \langle h| \otimes L_+^\mu([s_2, s'_2])$ between ancilla p_1 and system qudit $[s_2, s'_2]$. The controlled movement back is similar. Hence, the controlled braiding can be carried out in the following steps:

1. Perform the projection operation $|e\rangle \langle e|$ on the qudit on edge $[s_1, s_2]$.

2. Perform controlled unitary gate $|h\rangle_{p_1}\langle h| \otimes F(s_1) + |e\rangle_{p_1}\langle e| \otimes 1_{|G|}$ between ancilla p_1 and ancilla s_1 followed by controlled unitary gate $|e\rangle_{p_1}\langle e| \otimes F(s_2) + |h\rangle_{p_1}\langle h| \otimes 1_{|G|}$ between ancilla p_1 and ancilla s_2 , where F is the Fourier transformation. Apply the controlled gauge transformations $\sum_g |g\rangle_{s_1}\langle g| \otimes A_g(s_1)$ and $\sum_g |g\rangle_{s_2}\langle g| \otimes A_g(s_2)$, measure ancillary qudits s_1 and s_2 in basis $|k_{[G]}\rangle$. For outcomes k_{s_1} and k_{s_2} , perform controlled two-qudit gate $|e\rangle_{p_1}\langle e| \otimes Z_{[G]}^{k_{s_2}}([s_1, s_2]) + |h\rangle_{p_1}\langle h| \otimes Z_{[G]}^{k_{s_1}}([s_1, s_2])$ between ancilla p_1 and system qudit $[s_1, s_2]$
3. Perform controlled two-qudit gate $|e\rangle_{p_1}\langle e| \otimes I([s_2, s'_2]) + |h\rangle_{p_1}\langle h| \otimes L_+^\mu([s_2, s'_2])$ between ancilla p_1 and system qudit $[s_2, s'_2]$.
4. Braid the quasi-particle at site x_3 around site x_i .
5. Apply $|e\rangle_{p_1}\langle e| \otimes I([s_2, s'_2]) + |h\rangle_{p_1}\langle h| \otimes L_+^{\mu-1}([s_2, s'_2])$ between ancilla p_1 and qudit $[s_2, s'_2]$, measure qudit $[s_1, s_2]$ in basis $|g\rangle : g \in G$. For outcome g_1 , perform controlled gauge transformation $|e\rangle_{p_1}\langle e| \otimes A_{g_1^{-1}}(s_2) + |h\rangle_{p_1}\langle h| \otimes A_{g_1}(s_1)$, then perform $A(s_2)$.

In order to prevent unwanted braiding caused by noise, we must locate anyons faraway from each other, and rely on long braiding operators for interference measurement of the topological states. In contrast, in a fusion measurement by closed ribbon projection, when we move two anyons close enough we can choose a very small closed ribbon and perform the corresponding projection operator once only. Therefore, generally speaking, the topological state interference measurement is much more expensive than the fusion measurement.

IV. PROOF-OF-PRINCIPLE DEMONSTRATION OF NON-ABELIAN STATISTICS AND TQC

Since the simulation of non-Abelian anyons is very challenging, we are interested in finding out the smallest system that is sufficient for the demonstration of non-Abelian statistics and TQC. Here, we consider the braiding of a pure magnetic charge around a pure electric charge, and the fusion of two pure electric charges. And by these two processes, braiding and fusion, one could demonstrate non-Abelian statistics and TQC.

The graph shown in Fig. 3 (a) is the smallest system for demonstration of a unitary TQC gate by anyon braiding. We choose site x_0 as our base site. The gauge transformation $A_g(s_0)$ at s_0 is the smallest closed ribbon operator around s_0 . And $A_g(s_0)$ can also be viewed as creating a pure magnetic charge g , braiding it clockwise around vertex s_0 and annihilating it, we denote this braiding process as \mathcal{R}_1 . If initially there are only pure electric charge anyons in the system, then \mathcal{R}_1 corresponds to a braiding process surrounding the excitation at base site x_0 (pure electric charge anyons live on vertices). Now we consider the process that one create a pure magnetic charge g , counterclockwise braid it around all anyonic excitations in the system (excluding the excitation at base site x_0) and annihilate it, we denote this braiding process as \mathcal{R}_2 . So, when initially there are only pure electric charge anyons in the system, $\mathcal{R}_1\mathcal{R}_2^{-1}$ corresponds to a clockwise braiding process around all excitations in the system (including the excitation at base site x_0). And obviously this braiding is trivial, i.e. $\mathcal{R}_1\mathcal{R}_2^{-1} = 1$ or equally $\mathcal{R}_1 = \mathcal{R}_2$.

To demonstrate the non-Abelian anyon braiding, we first prepare the system in the ground state

$$|GS\rangle \propto \sum_{g_1, g_2 \in S_3} |g_1^{-1}\rangle_1 |g_1^{-1}\rangle_2 |g_1 g_2^{-1}\rangle_3 |g_2\rangle_4 |g_2\rangle_5. \quad (12)$$

Then we create a pure electric charge anyon at site x_1 , or equally we can say that we create a pure electric charge anyon at vertex s_1 (because pure electric charge anyons live on vertices). And we braid a pure magnetic charge anyon around this pure electric charge anyon by applying a gauge transformation at s_0 . Finally we detect the change of the anyon state. The detection can be done by the anyonic interference method given above, we make controlled braiding of pure magnetic charge anyons around x_1 , but we need to repeat the controlled braiding many times to complete the detection. Here, in this small-scale system, we can reduce the required number of braiding to just one. Notice that the controlled braiding for detection is just the controlled gauge transformation at s_0 . For example, we create at site x_1 (i.e. at vertex s_1) the pure electric charge anyon in topological state

$$\begin{aligned} |0_{R_2}\rangle \propto & \sum_{g_1 g_2^{-1} = e} |g_1^{-1}\rangle_1 |g_1^{-1}\rangle_2 |e\rangle_3 |g_2\rangle_4 |g_2\rangle_5 + \\ & \sum_{g_1 g_2^{-1} = c_+} \zeta |g_1^{-1}\rangle_1 |g_1^{-1}\rangle_2 |c_+\rangle_3 |g_2\rangle_4 |g_2\rangle_5 + \\ & \sum_{g_1 g_2^{-1} = c_-} \zeta^* |g_1^{-1}\rangle_1 |g_1^{-1}\rangle_2 |c_-\rangle_3 |g_2\rangle_4 |g_2\rangle_5, \end{aligned} \quad (13)$$

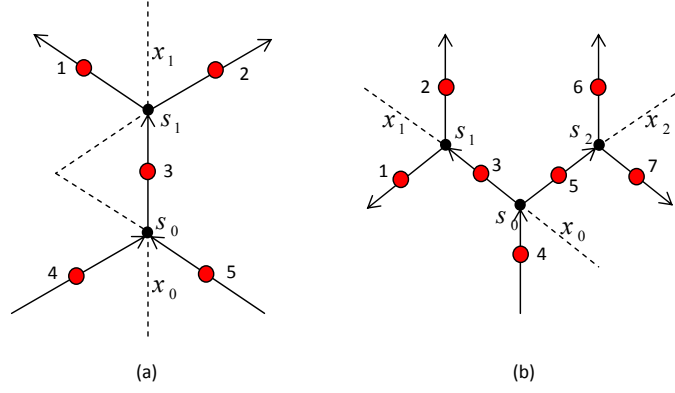


FIG. 3: (Color online) (a) The small-scale lattice with a minimum number of 5 system qudits (red[gray in black and white]) for demonstration of the non-Abelian anyon braiding. (b) The small-scale lattice with a minimum number of 7 system qudits (red[gray in black and white]) for the demonstration of non-Abelian anyon fusion.

where R_2 is the two dimensional irreducible representation of S_3 (the group elements and irreps of S_3 are given in the appendix). Then we apply the gauge transformation $A_{t_0}(s_0)$, which realizes the braiding unitary gate and transforms the anyon at site x_1 (i.e. at vertex s_1) to topological state $|1_{R_2}\rangle$ due to the braiding rules (see the appendix). To detect this change, we prepare the ancillary qudit at s_0 in state $\frac{1}{\sqrt{3}}(|e\rangle + |c_+\rangle + |c_-\rangle)$, apply controlled braiding $\sum_g |g\rangle_{s_0} \langle g| \otimes A_g(s_0)$, then measure the ancillary qudit s_0 in the Fourier basis $\{|j\rangle = \frac{1}{\sqrt{3}}(|e\rangle + \zeta^j |c_+\rangle + \zeta^{2j} |c_-\rangle)\}$, $j = 0, 1, 2$ where $\zeta = \exp(i2\pi/3)$. If the outcome is $|1\rangle$, the anyon state is $|0_{R_2}\rangle$. If the outcome is $|2\rangle$, the anyon state is $|1_{R_2}\rangle$. Else if the system is in ground state, the outcome must be $|0\rangle$. Note that the states of qudit 1 and qudit 2 are always the same in this whole demonstration. If we take the gauge transformation $A_g(s_0)$ as a single step, then the states of qudit 4 and qudit 5 are always the same too. Because of this, we can eliminate one of the duplicates from the physical simulator for simplification. We remove qudit 1 and 5.

For the small scale system in Fig. 3 (a), Fig. 4 (a) shows the detailed circuit for the described demonstration process. We only need one ancillary qudit s_0 for the measurement, so the total number of qudits for braiding demonstration is 4. Initially, all system qudits 2, 3, 4 are prepared in state $|e\rangle$, and ancilla s_0 is in state $\frac{1}{\sqrt{3}}(|e\rangle + |c_+\rangle + |c_-\rangle)$ for measurement. For ground state preparation, we need to perform symmetrized gauge transformation $A(s)$ Eq. 6 at s_0 and s_1 . Take $A(s_1)$ as an example, we can first transform qudit 2 to state $|0_{[S_3]}\rangle$ by Fourier transformation, then apply controlled unitary $\sum_g |g\rangle_2 \langle g| \otimes L_+^g(3)$. To create the anyon at x_1 , we first apply the projection $|e\rangle\langle e|$ on qudit 3. Then we need to perform the gauge transformations $A_e(s_1) + \zeta A_{c_+}(s_1) + \zeta^* A_{c_-}(s_1)$, this is done by first transforming qudit 3 to state $\frac{1}{\sqrt{3}}(|e\rangle + \zeta |c_+\rangle + \zeta^* |c_-\rangle)$ and then performing $\sum_g |g\rangle_3 \langle g| \otimes L_-^g(2)$. If we do not care about the ground state and only want to know the property of the state with anyonic excitations, we could directly prepare the system in the excited state as shown in Fig. 4 (c) to further simplify our scheme. We can rewrite the topological state $|0_{R_2}\rangle$ as

$$\begin{aligned}
 |0_{R_2}\rangle &\propto \sum_g |g^{-1}\rangle_2 |e\rangle_3 |g\rangle_4 + \\
 &\quad \sum_g \zeta |g^{-1} c_+^{-1}\rangle_2 |c_+\rangle_3 |g\rangle_4 + \\
 &\quad \sum_g \zeta^* |g^{-1} c_-^{-1}\rangle_2 |c_-\rangle_3 |g\rangle_4.
 \end{aligned}$$

To create this state, we first transform the system to state

$$\frac{1}{\sqrt{3}} |e\rangle_2 (|e\rangle_3 + \zeta |c_+\rangle_3 + \zeta^* |c_-\rangle_3) |0_{[S_3]}\rangle_4$$

by single qudit unitary, where $|0_{[S_3]}\rangle = |e\rangle + |c_+\rangle + |c_-\rangle + |t_0\rangle + |t_1\rangle + |t_2\rangle$. Then apply the controlled unitary $\sum_g |g\rangle_4 \langle g| \otimes L_-^g(2)$ followed by $\sum_g |g\rangle_3 \langle g| \otimes L_-^g(2)$. This is shown in Fig. 4 (c).

For the fusion measurement demonstration, we need more sites to place excitations. The graph shown in Fig. 3 (b) is the smallest system for demonstration of this elementary operation, where x_0 is the base site. We only consider the fusion measurement of pure electric charge excitations. We first prepare the system to ground state, then create

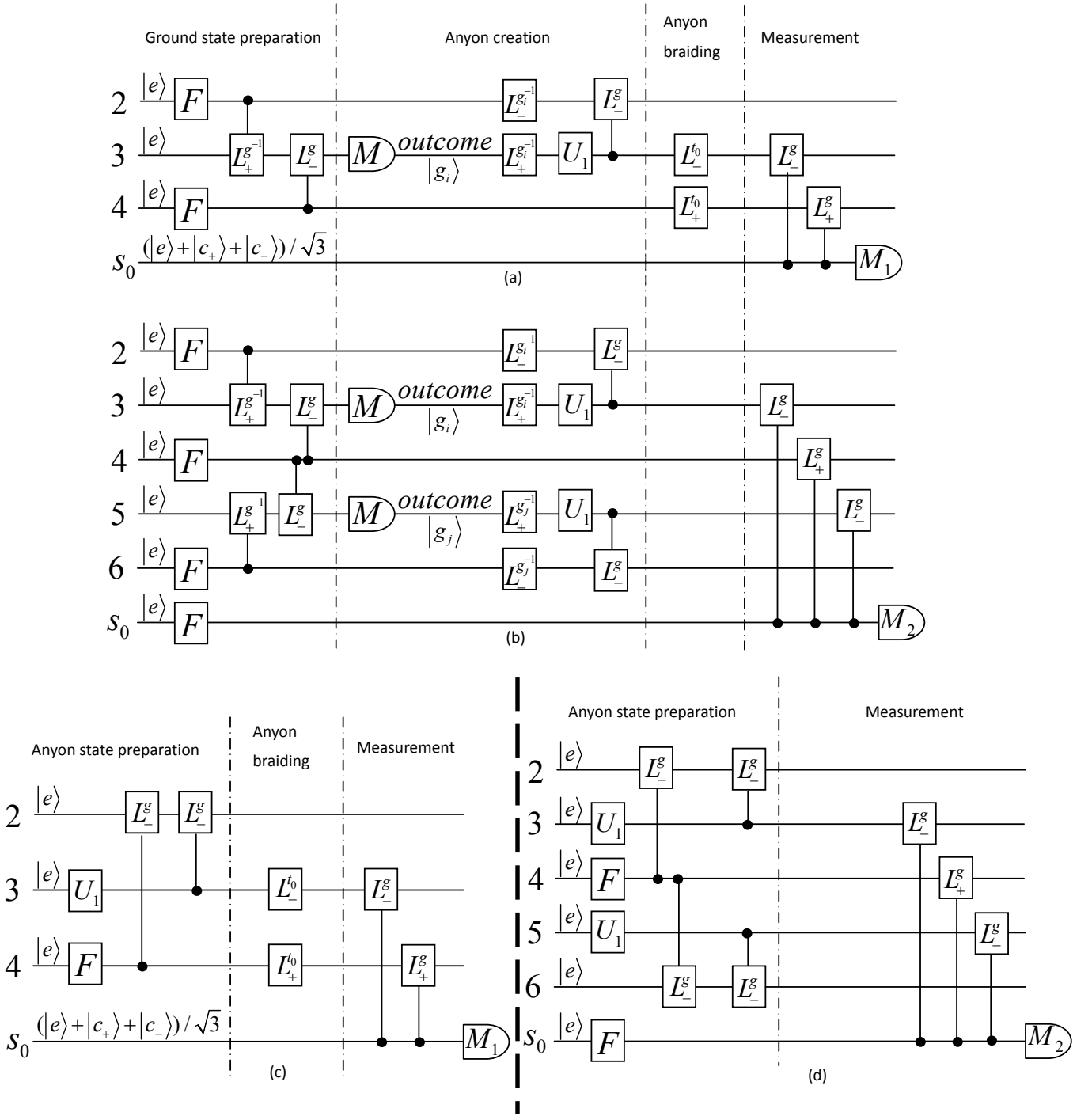


FIG. 4: The detailed quantum circuits for the demonstration of anyon braiding and measurement. The Fourier transformation F transforms state $|e\rangle$ to $|0_{[S_3]}\rangle$. The controlled $U_g = \sum_g |g\rangle_{control}\langle g| \otimes U_g(target)$. U_1 is a unitary operation that maps state $|e\rangle$ to $\frac{1}{\sqrt{3}}(|e\rangle + \zeta|c_+\rangle + \zeta^*|c_-\rangle)$, $\zeta = \exp(i2\pi/3)$. M , M_1 and M_2 are measurements in basis $\{|g\rangle\}$, $\{|k_{[z]}\rangle = Z_{[z]}^k|0_{[z]}\rangle, z = e, c_+, c_-\}$ and $\{|k_{[S_3]}\rangle = Z_{[S_3]}^k|0_{[S_3]}\rangle\}$. (a) is the quantum circuit for ground state preparation, anyon creation and braiding, and detection. (b) is the quantum circuit for ground state preparation, anyon creation and fusion detection. (c) and (d) are the corresponding quantum circuits with direct anyon state preparation.

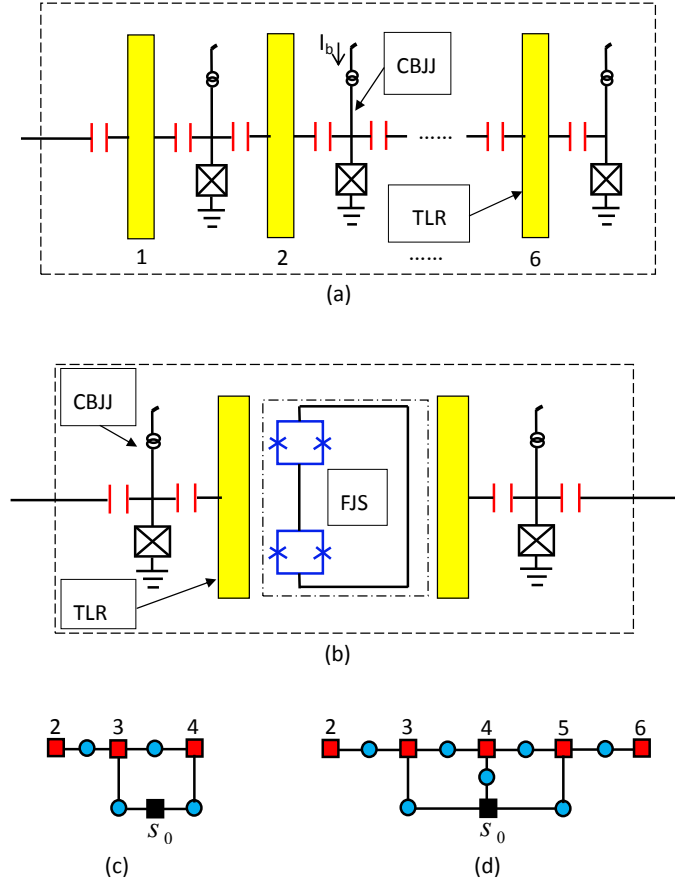


FIG. 5: (Color online)(a) A photonic qudit based on six TLRs that are capacitively coupled to current biased Josephson junction.(b) A 4-junction SQUID device is used to interact photonic qudits. (c)The superconducting circuit for demonstration of anyons braiding statistics. (d) The superconducting circuit for demonstration of the fusion of anyons. System qudits (red[gray in black and white] square) and ancillary qudits (black square) are coupled by the 4-junction SQUID (blue[gray in black and white] circle).

two arbitrary pure electric charge anyons at sites x_1 and x_2 (i.e. at vertices s_1 and s_2). Since there are only the two anyons in the system, and the total topological charge of all excitations in the system (including the excitation at base site) is vacuum. So iff there is no excitation at the base site x_0 , or equivalently iff the state of the system $|\psi\rangle$ satisfies $A(s_0)|\psi\rangle = |\psi\rangle$ (all excitations have no magnetic charge, so $B(p) \equiv 1$ for all p), the two pure electric charge anyons at s_1 and s_2 fuse to vacuum. So to detect the fusion, we prepare the ancillary qudit at s_0 in state $|0_{[S_3]}\rangle$, apply controlled gauge transformation $\sum_g |g\rangle_{s_0} \langle g| \otimes A_g(s_0)$, then measure the ancillary qudit s_0 in the basis $|k_{[S_3]}\rangle = Z_{[S_3]}^k |0_{[S_3]}\rangle$. If the outcome is $|0_{[S_3]}\rangle$, we get vacuum after fusion. Otherwise, we get a quasi-excitation left behind after fusion.

Since the states of qudit 1 and 2 are always the same in the whole process, so are those of qudit 6 and 7, we can eliminate qudits 1 and 7. Also we need an ancillary qudit s_0 for measurement, so the total number of qudits for fusion demonstration is 6. As an example, we can create two electric charge anyons in topological state $|0_{R_2}\rangle_{s_1} |0_{R_2}\rangle_{s_2}$, and measure their fusion. Based on the same consideration as the braiding demonstration, shown in Fig. 4 (b) and Fig. 4 (d) are the quantum circuits for this process with and without the ground state preparation respectively. Notice that the two anyons at s_1 and s_2 are in the same state $|0_{R_2}\rangle$, the operations on qudits 2,3 are the same as operations on 6,5 due to this symmetry.

Beside single qudit unitary operations on individual qudits, the above demonstration processes need two qudit gates between adjacent system qudits i and $i+1$. For measurement, we need two qudit gates between ancilla s_0 and system qudits 3, 4, 5.

For physical implementation, we can simulate this model using a variety of physical systems such as cold atoms or trapped ions. Here, we point out the interesting possibility of simulating it on a fully integrated superconducting chip which provides a powerful platform for manipulating and interacting photonic qubits based on on-chip transmission line (TLR) resonators [23]. We briefly describe the system only and leave the details to elsewhere. As shown in Fig. 5 [23], 6 transmission line resonators are used as 1 qudit. There is only 1 photon in the system of these 6 resonators and its location represents the 6 internal states of the qudit. By coupling the TLRs capacitively to current

biased Josephson junctions (CBBJ) as shown in Fig. 5 (a), we can shift the relative energies of the TLR modes and exchange photons between adjacent TLRs [23], and thus realize arbitrary single qudit gates. Further, we can use a four junction SQUID shown in Fig. 5 (b) to interact photons in 2 adjacent qudits to realize the 2-qudit phase gate $U = \exp(i\phi|g_i\rangle_A\langle g_i| \otimes |g_i\rangle_B\langle g_i|)$ [23]. Thus, we can perform all operations required to simulate the non-Abelian anyons in this system. Shown in Fig. 5 (c) and (d) are possible designs of the smallest superconducting circuits for the demonstration of anyon braiding and fusion measurement.

V. CONCLUSION

In summary, based on Kitaev's quantum double spin lattice model, we have proposed a method to simulate the non-Abelian statistics and universal TQC by performing appropriate ribbon operators. In contrast to earlier studies, our scheme is based on braiding of anyons created by long ribbon operators connected to a common base site, and hence can simulate genuine anyon states in a topologically protected global space. By designing the smallest system sufficient for the demonstration of fractional statistics and TQC, we have shown that the requirement of our proposal is only modest and it is an attractive scheme for experimental studies.

VI. ACKNOWLEDGMENTS

This work was funded by National Basic Research Program of China 2011CB921204, 2011CBA00200, National Natural Science Foundation of China (Grant Nos. 60921091, 10874170, 10875110, 11174270) and the Fundamental Research Funds for the Central Universities (Grant Nos. WK2470000006, WK2470000004). Z. -W. Zhou gratefully acknowledges the support of Research Fund for the Doctoral Program of Higher Education of China (Grant No.20103402110024) and the K. C. Wong Education Foundation, Hong Kong.

Appendix.A.

Some properties of the group S_3 :

S_3 , the group of permutations of three objects that we label 0,1,2, is the smallest non-Abelian group. S_3 contains three conjugacy classes, namely:

1. Identity e . Centralizer $N_{[e]} = S_3$.
2. Reflections $t_0 = (01)$, $t_1 = (12)$, $t_2 = (20)$. Centralizer $N_{[t_i]} \cong \{e, t_i\} \cong \mathbb{Z}_2$.
3. 3-rotations $c_+ = (012)$, $c_- = (021)$. Centralizer $N_{[c_i]} \cong \{e, c_+, c_-\} \cong \mathbb{Z}_3$.

The multiplication rules for S_3 are as follows:

$$\begin{aligned} t_i t_i &= e, t_j t_k = c_{\varepsilon_{j,k}}, \text{ for } j \neq k. \\ t_i c_{\pm} &= t_{i\pm 1}, c_{\pm} t_i = t_{i\mp 1}, \\ c_{\rho} c_{\rho} &= c_{-\rho}, c_{\rho} c_{\sigma} = e, \text{ for } \sigma \neq \rho. \end{aligned}$$

The operations involving e are trivial. Here $\varepsilon_{j,k} = \pm$ for $k = j \pm 1$ (modulo 3) respectively.

The group has three irreducible representations (irreps). Two one-dimensional irreps are the trivial one $R_1^+ = 1$, and the signature representation $R_1^-(e) = R_1^-(c_{\rho}) = +1$, $R_1^-(t_i) = -1$. The two dimensional representations are

$$R_2(e) = \mathbf{1}_2, R_2(t_k) = \sigma^x \exp(i\frac{2\pi}{3}k\sigma^z), R_2(c_{\pm}) = \exp(\pm i\frac{2\pi}{3}\sigma^z).$$

Explicitly,

$$\begin{aligned} R_2(e) &= \begin{pmatrix} 1 & 0 \\ 0 & 1 \end{pmatrix}, R_2(c_+) = \begin{pmatrix} \xi & 0 \\ 0 & \xi^* \end{pmatrix}, R_2(c_-) = \begin{pmatrix} \xi^* & 0 \\ 0 & \xi \end{pmatrix}, \\ R_2(t_0) &= \begin{pmatrix} 0 & 1 \\ 1 & 0 \end{pmatrix}, R_2(t_1) = \begin{pmatrix} 0 & \xi^* \\ \xi & 0 \end{pmatrix}, R_2(t_2) = \begin{pmatrix} 0 & \xi \\ \xi^* & 0 \end{pmatrix}, \end{aligned}$$

where $\xi = e^{i2\pi/3}$.

The characters $\chi_R(g) = \text{tr}[R(g)]$ are equal to ± 1 for one dimensional reps. For two dimensional reps,

$$\chi_{R_2}(e) = 2, \chi_{R_2}(t_i) = 0, \chi_{R_2}(c_\rho) = -1.$$

The permutation representation for S_3 is a set of 6×6 matrices that faithfully represents group left action on the basis $\{|e\rangle, |t_0\rangle, |t_1\rangle, |t_2\rangle, |c_+\rangle, |c_-\rangle\}$, i.e. $L_+^h|g\rangle = |hg\rangle$. Similarly the right multiplication $L_-^h|g\rangle = |gh^{-1}\rangle$, $[L_+^h, L_-^h] = 0$ and the unitary matrices are given by

$$L_+^e = \begin{pmatrix} 1 & 0 & 0 & 0 & 0 & 0 \\ 0 & 1 & 0 & 0 & 0 & 0 \\ 0 & 0 & 1 & 0 & 0 & 0 \\ 0 & 0 & 0 & 1 & 0 & 0 \\ 0 & 0 & 0 & 0 & 1 & 0 \\ 0 & 0 & 0 & 0 & 0 & 1 \end{pmatrix}, L_+^{t_0} = \begin{pmatrix} 0 & 1 & 0 & 0 & 0 & 0 \\ 1 & 0 & 0 & 0 & 0 & 0 \\ 0 & 0 & 0 & 0 & 1 & 0 \\ 0 & 0 & 0 & 0 & 0 & 1 \\ 0 & 0 & 1 & 0 & 0 & 0 \\ 0 & 0 & 0 & 1 & 0 & 0 \end{pmatrix},$$

$$L_+^{t_1} = \begin{pmatrix} 0 & 0 & 1 & 0 & 0 & 0 \\ 0 & 0 & 0 & 0 & 0 & 1 \\ 1 & 0 & 0 & 0 & 0 & 0 \\ 0 & 0 & 0 & 0 & 1 & 0 \\ 0 & 0 & 0 & 1 & 0 & 0 \\ 0 & 1 & 0 & 0 & 0 & 0 \end{pmatrix}, L_+^{t_2} = \begin{pmatrix} 0 & 0 & 0 & 1 & 0 & 0 \\ 0 & 0 & 0 & 0 & 1 & 0 \\ 0 & 0 & 0 & 0 & 0 & 1 \\ 1 & 0 & 0 & 0 & 0 & 0 \\ 0 & 1 & 0 & 0 & 0 & 0 \\ 0 & 0 & 1 & 0 & 0 & 0 \end{pmatrix},$$

$$L_+^{c_+} = \begin{pmatrix} 0 & 0 & 0 & 0 & 0 & 1 \\ 0 & 0 & 1 & 0 & 0 & 0 \\ 0 & 0 & 0 & 1 & 0 & 0 \\ 0 & 1 & 0 & 0 & 0 & 0 \\ 1 & 0 & 0 & 0 & 0 & 0 \\ 0 & 0 & 0 & 0 & 1 & 0 \end{pmatrix}, L_+^{c_-} = \begin{pmatrix} 0 & 0 & 0 & 0 & 1 & 0 \\ 0 & 0 & 0 & 1 & 0 & 0 \\ 0 & 1 & 0 & 0 & 0 & 0 \\ 0 & 0 & 1 & 0 & 0 & 0 \\ 0 & 0 & 0 & 0 & 0 & 1 \\ 1 & 0 & 0 & 0 & 0 & 0 \end{pmatrix},$$

$$L_-^e = \begin{pmatrix} 1 & 0 & 0 & 0 & 0 & 0 \\ 0 & 1 & 0 & 0 & 0 & 0 \\ 0 & 0 & 1 & 0 & 0 & 0 \\ 0 & 0 & 0 & 1 & 0 & 0 \\ 0 & 0 & 0 & 0 & 1 & 0 \\ 0 & 0 & 0 & 0 & 0 & 1 \end{pmatrix}, L_-^{t_0} = \begin{pmatrix} 0 & 1 & 0 & 0 & 0 & 0 \\ 1 & 0 & 0 & 0 & 0 & 0 \\ 0 & 0 & 0 & 0 & 0 & 1 \\ 0 & 0 & 0 & 0 & 1 & 0 \\ 0 & 0 & 0 & 1 & 0 & 0 \\ 0 & 0 & 1 & 0 & 0 & 0 \end{pmatrix},$$

$$L_-^{t_1} = \begin{pmatrix} 0 & 0 & 1 & 0 & 0 & 0 \\ 0 & 0 & 0 & 0 & 1 & 0 \\ 1 & 0 & 0 & 0 & 0 & 0 \\ 0 & 0 & 0 & 0 & 0 & 1 \\ 0 & 1 & 0 & 0 & 0 & 0 \\ 0 & 0 & 0 & 1 & 0 & 0 \end{pmatrix}, L_-^{t_2} = \begin{pmatrix} 0 & 0 & 0 & 1 & 0 & 0 \\ 0 & 0 & 0 & 0 & 0 & 1 \\ 0 & 0 & 0 & 0 & 1 & 0 \\ 1 & 0 & 0 & 0 & 0 & 0 \\ 0 & 0 & 1 & 0 & 0 & 0 \\ 0 & 1 & 0 & 0 & 0 & 0 \end{pmatrix},$$

$$L_-^{c_+} = \begin{pmatrix} 0 & 0 & 0 & 0 & 1 & 0 \\ 0 & 0 & 1 & 0 & 0 & 0 \\ 0 & 0 & 0 & 1 & 0 & 0 \\ 0 & 1 & 0 & 0 & 0 & 0 \\ 0 & 0 & 0 & 0 & 0 & 1 \\ 1 & 0 & 0 & 0 & 0 & 0 \end{pmatrix}, L_-^{c_-} = \begin{pmatrix} 0 & 0 & 0 & 0 & 0 & 1 \\ 0 & 0 & 0 & 1 & 0 & 0 \\ 0 & 1 & 0 & 0 & 0 & 0 \\ 0 & 0 & 1 & 0 & 0 & 0 \\ 1 & 0 & 0 & 0 & 0 & 0 \\ 0 & 0 & 0 & 0 & 1 & 0 \end{pmatrix}.$$

Further, the group S_3 has a semi-direct product structure which may be exploited to simplify physical realizations. We have $S_3 \cong \mathbb{Z}_3 \rtimes_\phi \mathbb{Z}_2 = \{a, b | a^3 = e, b^2 = e, \phi : \phi_b(a) = bab^{-1} = a^2\}$. We can choose $\mathbb{Z}_3 = \{e, c_+, c_-\}$, $\mathbb{Z}_2 = \{e, t_0\}$, and any element $g \in S_3$ can be written as $g = c_+^r t_0^s$ for $r \in \{0, 1, 2\}$, $s \in \{0, 1\}$. The above unitary matrices can be simplified in $\{|r\rangle|s\rangle \equiv |c_+^r t_0^s\rangle\}$, a product basis for a qutrit and qubit [16].

$$\begin{aligned}
L_+^e &= 1_3 \otimes 1_2, L_+^{t_0} = F(1, 2) \otimes \sigma^x, L_+^{t_1} = F(0, 2) \otimes \sigma^x, \\
L_+^{t_2} &= F(0, 1) \otimes \sigma^x, L_+^{c_+} = X^{-1} \otimes 1_2, L_+^{c_-} = X \otimes 1_2, \\
L_-^e &= 1_3 \otimes 1_2, L_-^{t_0} = 1_3 \otimes \sigma^x, \\
L_-^{t_1} &= X^{-1} \otimes \sigma^- + X \otimes \sigma^+, L_-^{t_2} = X^{-1} \otimes \sigma^+ + X \otimes \sigma^-, \\
L_-^{c_+} &= X^{-1} \otimes |0\rangle\langle 0| + X \otimes |1\rangle\langle 1|, \\
L_-^{c_-} &= X \otimes |0\rangle\langle 0| + X^{-1} \otimes |1\rangle\langle 1|,
\end{aligned}$$

where $F(i, j) = (|i\rangle\langle j| + |j\rangle\langle i|) \oplus 1$ flip two basis states of qutrit, and $X = \sum_i |i+1\rangle\langle i|$.

Appendix.B.

Some properties of the $D(S_3)$ anyons :

The types of the quasi-particle of the Quantum Double model have a 1-to-1 correspondence with irreducible representations of $D(G)$. The 8 irreps for $D(S_3)$ and the corresponding quantum dimensions are:

- Vacuum $\Pi_{R_1^+}^{[e]}, d = 1$;
- Pure electric charges $\Pi_{R_1^-}^{[e]}, \Pi_{R_2}^{[e]}, d = 1, 2$;
- Pure magnetic charges $\Pi_{\beta_0}^{[c]}, \Pi_{\gamma_0}^{[t]}, d = 2, 3$;
- Dyonic combinations $\Pi_{\beta_1}^{[c]}, \Pi_{\beta_2}^{[c]}, \Pi_{\gamma_1}^{[t]}, d = 2, 2, 3$,

where γ_0, γ_1 correspond to the identity and signature representation of $N_{[t]} \cong \{e, t_0\} \cong \mathbb{Z}_2$. $\beta_0, \beta_1, \beta_2$ are the three one dimensional irreps of $N_{[c]} \cong \{e, c_+, c_-\} \cong \mathbb{Z}_3$. β_0 is the identity representation. Here we only give braiding rules of the pure charge excitations, a full description can be found in [6, 19].

$$\begin{aligned}
\mathcal{R}|\nu_1\rangle|\nu_2\rangle &= |\nu_1\nu_2\nu_1^{-1}\rangle|\nu_1\rangle, \\
\mathcal{R}^2|\nu\rangle|\xi_n^R\rangle &= |\nu\rangle|R(\nu)_{mn}\xi_m^R\rangle,
\end{aligned}$$

where R is the unitary irrep of S_3 and ξ_n^R corresponding to pure electric charge excitation, ν corresponds to pure magnetic charge, \mathcal{R} represents the counterclockwise exchange of the two anyonic excitations. The exchange between pure electric charges is trivial.

-
- [1] F. Wilczek, Phys. Rev. Lett. **48**, 1144 (1982).
[2] X.-G. Wen, *Quantum Field Theory of Many-Body Systems* (Oxford University, Oxford, 2004).
[3] V. J. Goldman and B. Su, Science **267**, 1010 (1995).
[4] F. E. Camino, W. Zhou, and V. J. Goldman, Phys. Rev. Lett. **95**, 246802 (2005).
[5] F. E. Camino, W. Zhou, and V. J. Goldman, Phys. Rev. B **72**, 075342 (2005).
[6] A. Kitaev, Ann. Phys. (N.Y.) **303**, 2 (2003).
[7] A. Kitaev, cond-mat/0506438.
[8] S. Das Sarma, M. Freedman, and C. Nayak, Phys. Rev. Lett. **94**, 166802 (2005).
[9] P. Bonderson, A. Kitaev, and K. Shtengel, Phys. Rev. Lett. **96**, 016803 (2006).
[10] L.-M. Duan, E. Demler, and M. D. Lukin, Phys. Rev. Lett. **91**, 090402 (2003).
[11] A. Micheli, G. K. Brennen, and P. Zoller, Nature Phys. **2**, 341 (2006).
[12] C.-W. Zhang, *et al.*, quant-ph/0609101; J. K. Pachos, quant-ph/0605068.
[13] Y.-J. Han, R. Raussendorf, and L.-M. Duan, Phys. Rev. Lett. **98**, 150404 (2007).
[14] C.-Y. Lu, Wei-Bo. Gao, O. Guhne, X.-Q. Zhou, Z.-B. Chen, and J-Wei Pan, Phys. Rev. Lett. **102**, 030502 (2009).
[15] M. Aguado, G. K. Brennen, F. Verstraete, J. I. Cirac, Phys. Rev. Lett. **101**, 260501 (2008).
[16] G. K. Brennen, M. Aguado, J. I. Cirac, arXiv:quant-ph/09011345v1.

- [17] D. W. Berry, M. Aguado, A. Gilchrist, and G. K. Brennen, arXiv:quant-ph/09064578v2.
- [18] J. R. Wooton, V. Lahtinen, and J. K. Pachos, LNCS 5906, 56 (2009).
- [19] M. de Wild Propitius, *Topological interactions in broken gauge theories*, PhD thesis, University of Amsterdam, 1995.
- [20] C. Mochon, Phys. Rev. **A69**, 032306 (2004).
- [21] G. K. Brennen, D. P. O'Leary, and S. S. Bullock, Phys. Rev. **A71**, 052318 (2005).
- [22] H. Bombin, M. A. Martin-Delgado, Phys. Rev. **B78**, 115421 (2008).
- [23] Lianghu Du *et al* New. J. Phys. **12**, 063015 (2010).